

## REPORT 1025

# EXPERIMENTAL AND THEORETICAL STUDIES OF AREA SUCTION FOR THE CONTROL OF THE LAMINAR BOUNDARY LAYER ON AN NACA 64A010 AIRFOIL<sup>1</sup>

By ALBERT L. BRASLOW, DALE L. BURROWS, NEAL TETERVIN, and FIORAVANTE VISCONTI

### SUMMARY

A low-turbulence wind-tunnel investigation was made of an NACA 64A010 airfoil having a porous surface to determine the reduction in section total-drag coefficient that might be obtained at large Reynolds numbers by the use of suction to produce continuous inflow through the surface of the airfoil (area suction). In addition to the experimental investigation, a related theoretical analysis was made to provide a basis of comparison for the test results.

Full-chord laminar flow was maintained by application of area suction up to a Reynolds number of approximately  $20 \times 10^6$ . At this Reynolds number, combined wake and suction drags of the order of 38 percent of the drag for a smooth and fair NACA 64A010 airfoil without boundary-layer control were obtained. The minimum experimental values of suction-flow coefficient for full-chord laminar flow were of the same order of magnitude as the theoretical values and decreased with an increase in Reynolds number in the same manner as the theoretical values. It seems likely from the results that attainment of full-chord laminar flow by means of continuous suction through a porous surface will not be precluded by a further increase in Reynolds number provided that the airfoil surfaces are maintained sufficiently smooth and fair and provided that outflow of air through the surface is prevented.

Although area suction was able to overcome the destabilizing effects of an adverse pressure gradient such as that which occurs over the rear portion of an airfoil, area suction does not appear to stabilize the boundary layer completely for relatively large disturbances such as those which might be caused by protuberances that have a height comparable to the boundary-layer thickness.

### INTRODUCTION

The stability theory for the incompressible laminar boundary layer is an analysis of the damping or amplification of vanishingly small two-dimensional aerodynamically possible disturbances in the boundary layer (reference 1). A possible definition in the physical sense of a small disturbance is one that does not produce transition from laminar to turbulent flow at its origin in contrast with a large

disturbance, which does cause immediate transition. Small disturbances may either amplify as they progress downstream and eventually grow large enough to cause turbulence or they may be damped and cause no change in the downstream flow; if small disturbances of all frequencies are damped rather than amplified, the laminar boundary layer is considered stable (reference 2).

Theoretical investigations have been made of the characteristics of flows past a flat plate through which there is a small normal velocity and, in addition, the stability theory has been used to calculate the stability of the laminar boundary layer for this type of flow. Examples of some of this theoretical work can be found in references 3 to 7 and in British work (not generally available). The results of these analyses indicate that a small normal velocity into the surface at all points along the surface has a large stabilizing effect on the laminar layer. Inasmuch as there appear to be no data that show this effect experimentally, an investigation of the effect of area suction on the boundary-layer stability is being made in the Langley low-turbulence pressure tunnel. Three suction arrangements were investigated on an NACA 64A010 airfoil that had porous sintered-bronze surfaces. Measurements were made up to a Reynolds number of approximately  $20 \times 10^6$  and included wake drags, suction-flow quantities, suction losses, and a few boundary-layer velocity profiles.

In order to provide a basis of comparison for the measured suction flows, the stability of the laminar boundary layer was calculated for two important cases of chordwise suction distribution for the test airfoil. Theoretical results are also presented for a flat plate with uniform suction. The calculations were made by combining Schlichting's theory for the computation of the laminar boundary layer (reference 8) with Lin's theory for the determination of the stability of the laminar velocity profile (reference 1). Suction quantities necessary to keep the boundary layer neutrally stable at all points along the airfoil chord were calculated for Reynolds numbers of  $6 \times 10^6$ ,  $15 \times 10^6$ , and  $25 \times 10^6$ . The minimum suction quantities required to keep the boundary layer stable were obtained also for the case where the inflow velocity is constant over the entire surface.

<sup>1</sup> Supersedes NACA TN 1905, "Experimental and Theoretical Studies of Area Suction for the Control of the Laminar Boundary Layer on a Porous Bronze NACA 64A010 Airfoil" by Dale L. Burrows, Albert L. Braslow, and Neal Tetervin, 1949, and NACA TN 2112, "Further Experimental Studies of Area Suction for the Control of the Laminar Boundary Layer on a Porous Bronze NACA 64A010 Airfoil" by Albert L. Braslow and Fioravante Visconti, 1950.

## SYMBOLS

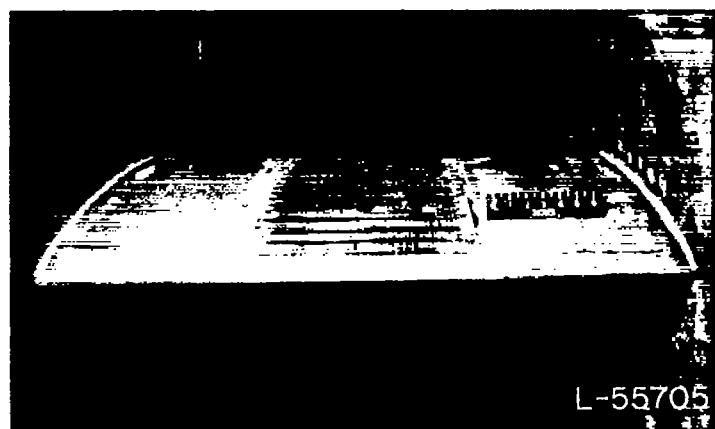
$\alpha_0$	section angle of attack
$c$	airfoil chord
$b$	span of porous surface
$x$	distance along chord from leading edge of airfoil
$s$	distance along surface from leading edge of airfoil
$y$	distance normal to surface of airfoil
$\rho_0$	free-stream mass density
$U_0$	free-stream velocity
$q_0$	free-stream dynamic pressure $\left(\frac{1}{2} \rho_0 U_0^2\right)$
$U$	local velocity parallel to surface at outer edge of boundary layer
$u$	local velocity parallel to surface and inside boundary layer
$Q$	total quantity rate of flow through both airfoil surfaces
$C_Q$	suction-flow coefficient $\left(\frac{Q}{bcU_0}\right)$
$H_0$	free-stream total pressure
$H_t$	total pressure in model interior
$p$	local static pressure on airfoil surface
$S$	airfoil pressure coefficient $\left(\frac{H_0 - p}{q_0}\right)$
$R$	free-stream Reynolds number based on airfoil chord
$C_P$	suction-air pressure-loss coefficient $\left(\frac{H_0 - H_t}{q_0}\right)$
$c_{d_w}$	section wake-drag coefficient
$c_{d_s}$	section suction-drag coefficient $(C_Q C_P)$
$c_{d_T}$	section total-drag coefficient $(c_{d_s} + c_{d_w})$
$\delta^*$	displacement thickness $\left(\int_0^\infty \left(1 - \frac{u}{U}\right) dy\right)$
$\theta$	momentum thickness $\left(\int_0^\infty \frac{u}{U} \left(1 - \frac{u}{U}\right) dy\right)$
$R_{\delta^*} = \frac{U \delta^*}{\nu}$	
$\nu$	kinematic viscosity
$v_0$	velocity through airfoil surface (for suction, $v_0 < 0$ ; for blowing, $v_0 > 0$ )
$\Delta p$	static pressure drop across porous surface
$c_{v_0}$	porosity factor, $\text{length}^2 \left(\left \frac{v_0}{\Delta p}\right  \mu t\right)$
$\mu$	absolute viscosity
$t$	thickness of porous material
$z = \left(\frac{\theta}{c}\right)^2 \frac{U_0 c}{\nu}$	(reference 8)
$G$	function of $k$ and $k_1$ (reference 8)
$k = z \frac{dU}{d\frac{s}{c}}$	(reference 8)
$k_1 = f_1 \sqrt{z}$	(reference 8)
$f_1 = \frac{-v_0}{U_0} \sqrt{\frac{U_0 c}{\nu}}$	(reference 8)

$K$	profile shape parameter (reference 8)
$\eta = \frac{y}{\delta_1}$	(reference 8)
$\delta_1$	measure of boundary-layer thickness (reference 8)
$u_c$	velocity of disturbance in boundary layer
$R_{\delta^*_{cr}}$	value of $R_{\delta^*}$ at which disturbance is neither damped nor amplified

## MODEL

Photographs of the 3-foot-chord by 3-foot-span model mounted in the Langley low-turbulence pressure tunnel are presented as figure 1. The model was formed to the NACA 64A010 profile, ordinates for which are presented in reference 9. The theoretical pressure distribution of this airfoil at zero angle of attack is presented in figure 2.

A sketch showing the details of the model construction is presented as figure 3. The model was constructed with two hollow cast-aluminum end sections which were machined to contour and connected to an under-contour hollow center casting that served as a base support for the bronze skin. The skin was directly supported on a chordwise arrangement of  $\frac{1}{4}$ -inch spanwise rods which were attached to the under-contour casting. The chordwise locations of these rods are



(a) Leading edge.



(b) Trailing edge.

FIGURE 1.—NACA 64A010 airfoil model with porous sintered-bronze surface mounted for area-suction studies in Langley low-turbulence pressure tunnel.

shown as figure 4. This arrangement of support rods, in which the rods made essentially line contact with the skin, was intended to provide as much open area as possible on the inner side of the skin so that very little of the skin would be blanked off from the suction flow. The center casting was perforated with 1-inch holes over the center portion and 1-inch slits at the model leading and trailing edges to provide a passageway for the air from the skin into the inner chamber of the hollow casting. This model configuration is herein referred to as configuration 1.

The model was made such that the chordwise flow could be altered by installing orifices in the model base casting as shown in figure 4. Flow between compartments formed by the  $\frac{1}{4}$ -inch rods could be prevented by sealing the rods to

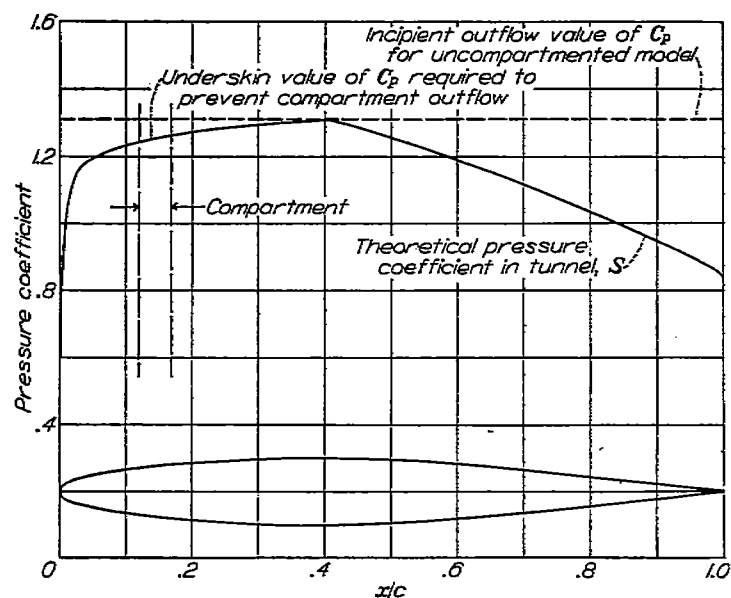


FIGURE 2.—External-pressure and suction-pressure distributions for porous bronze NACA 64A010 airfoil model.  $\alpha = 0^\circ$ .

the skin with rubber cement. The model arrangement with orifices and compartment seal is referred to herein as configuration 2. A photograph which shows model configuration 2 with the skin removed is shown as figure 5.

For configurations 1 and 2, the upper and lower surfaces of the 13-inch center section of the span were constructed from a continuous sheet of porous sintered bronze with a single spanwise joint at the model trailing edge, which was fastened only at the spanwise edges to  $\frac{1}{4}$ -inch inner end plates; consequently, a 12-inch span of the skin was left open to suction. In order to prevent outflow from the upper and lower leading-edge compartments, the leading-edge skin of configuration 2 was saturated with lacquer for a distance of 1 inch ( $\frac{s}{c} = 0.028$ ) from the leading edge on both upper and lower surfaces.

A third suction arrangement was investigated (configuration 3) wherein the orifices in the model base casting were removed and a low-porosity skin was installed. Flow between compartments was not prevented by sealing the rods to the skin. Two bronze sheets were used to form the center part of the airfoil surfaces from the trailing edge to the 2-percent-chord station. A sheet of duralumin was formed around the leading-edge contour and butted to the bronze. The skin was fastened at the butt joint in addition to being fastened along the spanwise edges to the  $\frac{1}{4}$ -inch inner end plates; the leading edge was glazed and faired with hard-drying putty up to the 5-percent-chord station.

The same sintered-bronze sheet was used in configurations 1 and 2 and was fabricated of spherical bronze powder that was specified to be small enough to pass through a 200-mesh screen but too large to pass through a 400-mesh screen. The thickness of the sheet was found to vary about  $\pm 0.010$  inch from a mean of 0.080 inch. The sintered-bronze sheets of configuration 3 were approximately 0.090-inch thick and

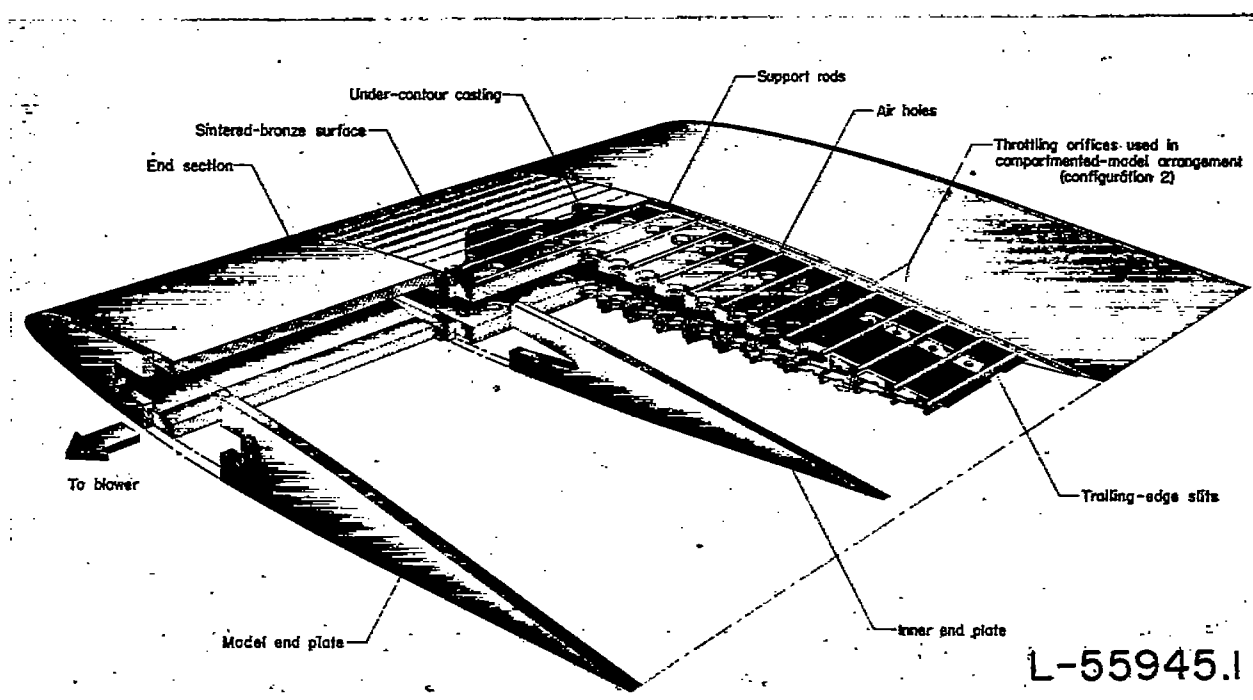


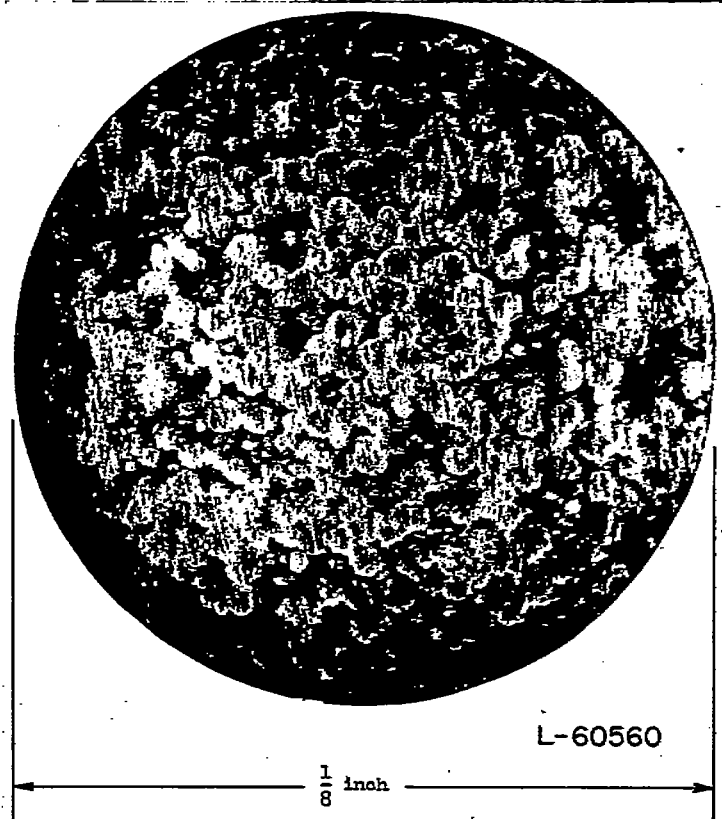
FIGURE 3.—Construction of porous bronze NACA 64A010 airfoil model.

L-55945.1



The porosity of the sintered-bronze material was such that the flow quantity varied directly with the pressure drop, as is characteristic of dense filters. With air at standard conditions the measured porosity of the skin of configurations 1 and 2 and the skin of configuration 3 was such that an applied suction of 0.06 and of 1.84 pounds per square inch, respectively, induced a velocity of 0.5 foot per second through the material; these values amount to porosity factors  $c_r$  equal

As a result of a low modulus of elasticity of the material and the variations in thickness, the airfoil contour of configurations 1 and 2 as tested was quite wavy. Absolute variations from the true profile were not measured; however,



(a) Representative of approximately 80 percent of total area.

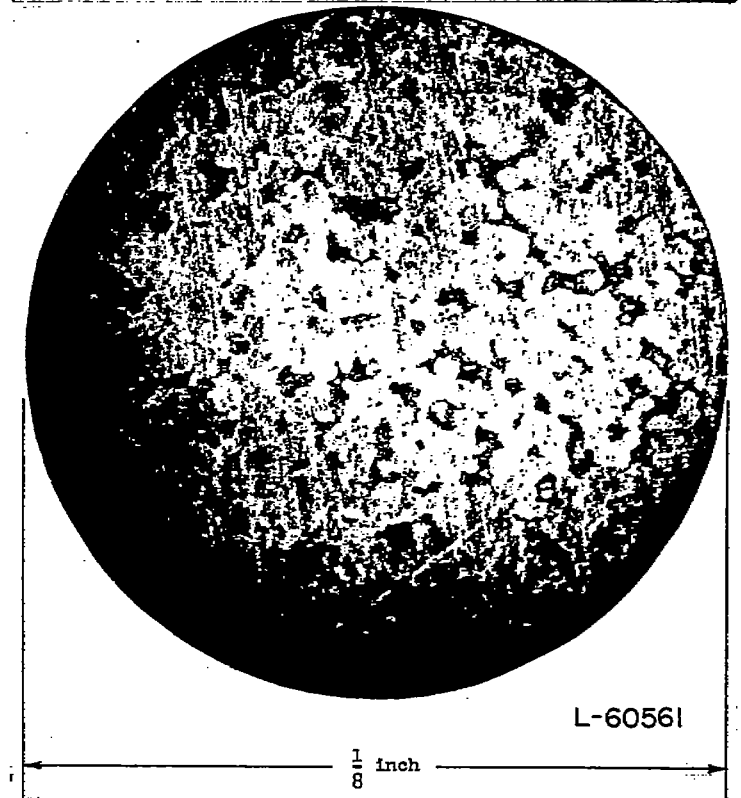
FIGURE 6.—Photomicrographs of sanded sintered-bronze surface as tested.

a relative waviness survey was made at various spanwise stations with a three-point indicating mechanism (fig. 7). An estimate of the degree of waviness of the bronze surface may be obtained by comparing the profiles for the bronze surface with the profiles of the cast-aluminum end sections; the profiles of the end sections varied no more than  $\pm 0.003$  inch from the true airfoil profile. No waviness survey was made on model configuration 3; however, the surfaces were somewhat smoother and fairer than the surfaces of configurations 1 and 2.

#### APPARATUS AND TESTS

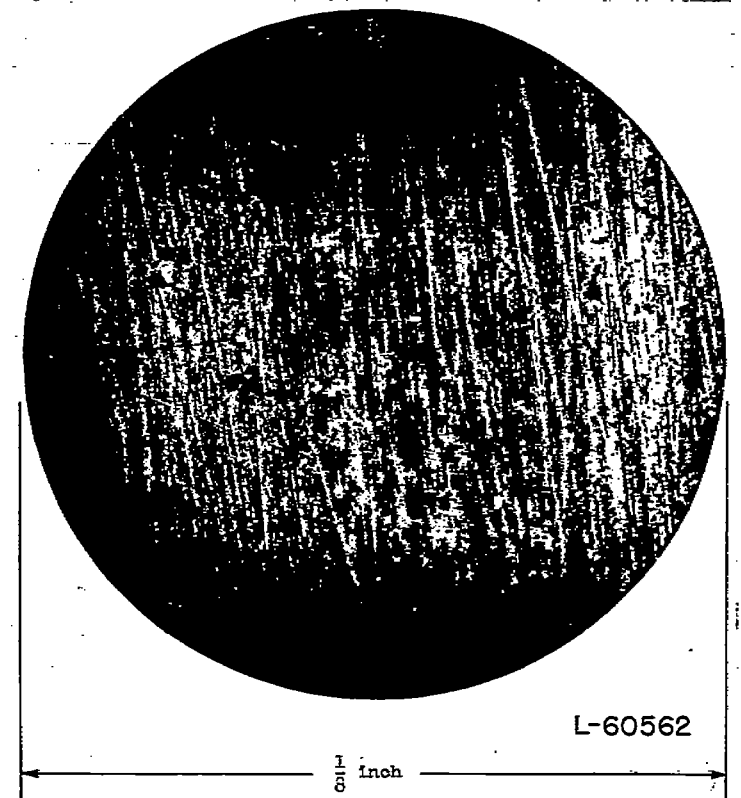
The model was tested in the Langley low-turbulence pressure tunnel and was mounted as shown in figure 1. A detailed description of this tunnel is given in reference 10. Flow measurements for the suction air were made by means of an orifice plate in the suction duct. The suction flow was taken through one of the model end plates and was regulated by varying the blower speed and the diameter of the orifice which was used to measure suction flow.

A static-pressure tube was used to measure the suction pressure in the inner compartment of the center casting. Since the velocity was low, the measured static pressure was very nearly equal to the total pressure. These data were used to obtain the total pressure lost by the suction air in passing from the free stream to the inner chamber of the model and were also used to give an indication of outflow which occurred when the pressure inside the model was greater than the lowest pressure on the airfoil surface.



(b) Representative of approximately 19 percent of total area.

FIGURE 6.—Continued.



(c) Representative of approximately 1 percent of total area.

FIGURE 6.—Concluded.

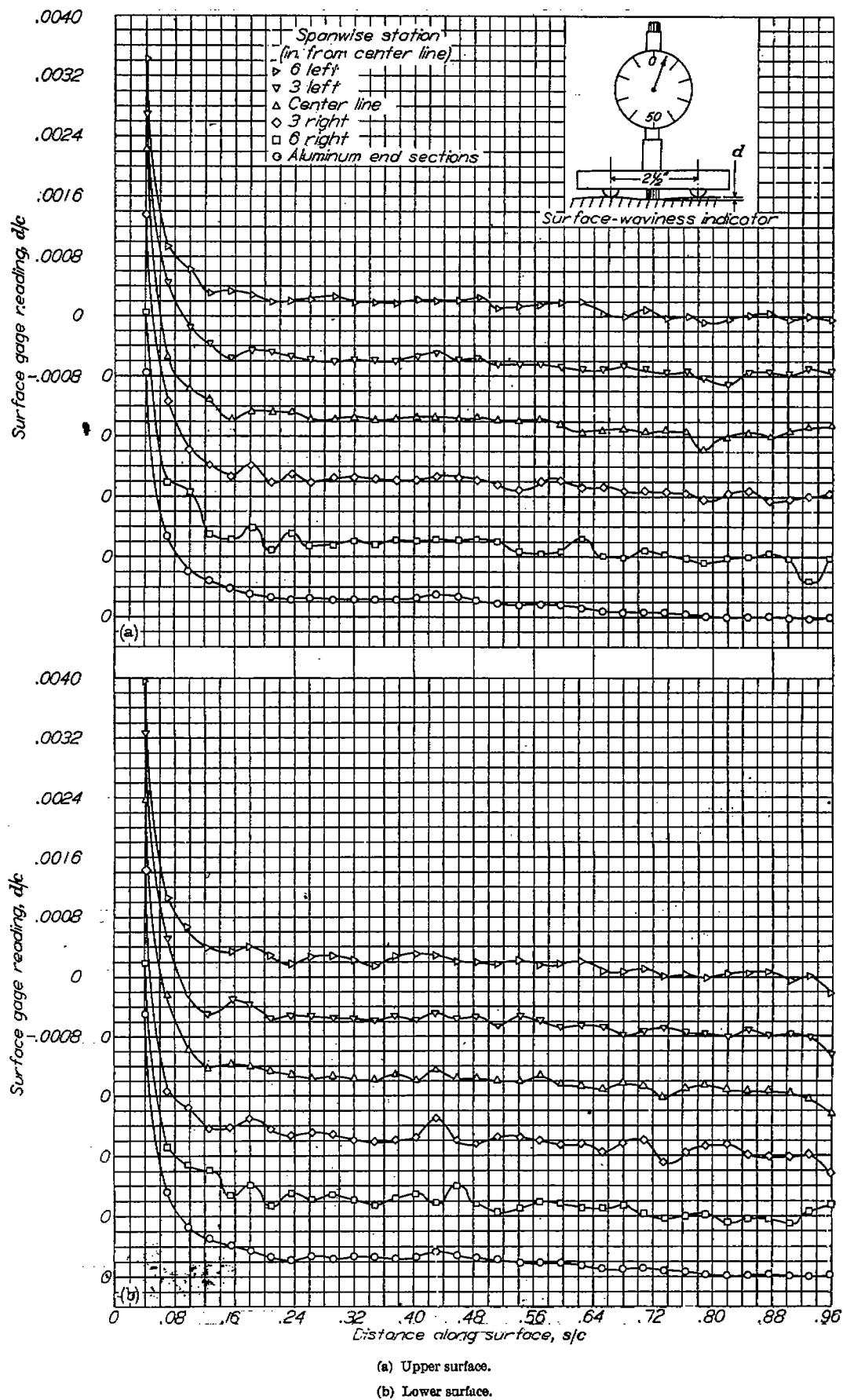


FIGURE 7.—Chordwise surface-waviness survey for various spanwise positions across porous bronze NACA 64A010 airfoil model. Configurations 1 and 2.

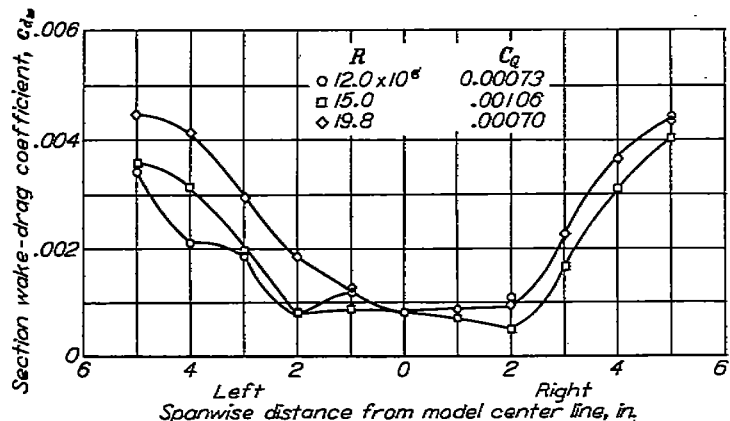


FIGURE 8.—Spanwise variation of section wake-drag coefficient on porous bronze NACA 64A010 airfoil model for three Reynolds numbers and suction-flow coefficients.  $\alpha = 0^\circ$ ; configuration 3.

For configurations 1 and 3, the skin was the only resistance to the suction; that is, air passages between the skin and the inner chamber were large enough to make the internal losses low in comparison with the pressure drop through the skin. The use of flow-control orifices in each compartment of configuration 2 had the disadvantage that any one set of orifices such as shown in figure 4 was able to produce a near-uniform chordwise inflow distribution only at free-stream Reynolds numbers below the design value, which for this case was  $6.0 \times 10^6$ . No attempt was made to measure the flow in each compartment because of the exploratory nature of the tests. To obtain an indication of outflow through the skin, however, the suction pressure was measured in compartment 5 under the upper-surface skin (fig. 4). Because of the peculiarities of the throttling system, calculations indicated that compartment 5 would be the most critical to outflow.

Spanwise surveys of section wake-drag coefficient over the part of the model covered with the porous skin indicated appreciable variations in wake drag. Examples of these variations are shown in figure 8 for configuration 3. The large variations, occurring only over the outer portions of the bronze skin, were due to disturbances originating at or near the junctures between the bronze skin and the solid model end sections; over a spanwise region of approximately 4 inches at the center of the bronze skin, the measured wake-drag coefficients were rather constant. The wake drags and boundary-layer measurements presented herein were obtained at the center region of the model and are believed to correspond to the true two-dimensional conditions and to be essentially uninfluenced by the flow disturbances outside this region. All wake drags were measured with a survey rake located at about 70 percent of the chord behind the model trailing edge. Boundary-layer measurements were obtained with a conventional multitube "mouse" (reference 11) located on the center line of the upper surface of configuration 1 at 83 percent of the chord. Station 0.83c was the most rearward position at which the mouse could be mounted conveniently. The tests were made for Reynolds numbers up to  $19.8 \times 10^6$  and for suction-flow coefficients up to 0.01 with the model set at zero angle of attack.

## RESULTS AND DISCUSSION

### THEORETICAL

In order to provide a standard of comparison for the experimental results, the characteristics of the laminar boundary layer were calculated for flow into the surface of the NACA 64A010 airfoil at an angle of attack of  $0^\circ$ . The minimum suction quantities necessary to keep the laminar boundary layer neutrally stable over the entire surface at Reynolds numbers of  $6 \times 10^6$ ,  $15 \times 10^6$ , and  $25 \times 10^6$  were computed. The stability of the boundary layer was also investigated for cases in which the velocity through the surface was everywhere the same.

The boundary-layer velocity profiles and thicknesses were calculated by the Schlichting method (reference 8), an approximate method. The velocity profiles of the Schlichting method are a single-parameter family of curves for which the parameter depends on the velocity of flow into the surface, the pressure gradient along the surface, the boundary-layer thickness, and the kinematic viscosity of the fluid. The single-parameter family of velocity profiles is used with the boundary-layer-momentum equation to obtain a first-order differential equation. In the calculations, the differential equation of reference 8 was integrated by Euler's step-by-step method. In the process of integrating the differential equation, the boundary-layer profiles and boundary-layer thicknesses are found at each point along the wing surface. The lengths of the steps in the integration process were about the same for all the calculations and were so small that halving them made no important difference for the no-suction case and a Reynolds number of  $25 \times 10^6$ .

In order to begin the calculation, the value of  $\frac{dz}{ds}$ , the rate of change of a representative boundary-layer-thickness parameter, at  $x=0$  (reference 8) was taken as zero. This value of  $\frac{dz}{ds}$  was found from the equation

$$\left(\frac{dz}{ds}\right)_{\frac{s}{c} \rightarrow 0} = \left[ \frac{z \left( \frac{d^2 U/U_0}{ds/c^2} \right) \frac{\partial G}{\partial k} + \frac{df_1}{ds/c} \sqrt{z} \frac{\partial G}{\partial k_1}}{\frac{dU/U_0}{ds/c} \left( 1 - \frac{\partial G}{\partial k} \right) - \frac{f_1}{2} \frac{\partial G}{\partial k_1} \frac{1}{\sqrt{z}}} \right]_{\frac{s}{c} \rightarrow 0}$$

which was obtained by applying L'Hospital's Rule to the equation for  $\frac{dz}{ds}$ , equation (30) of reference 8. In order to continue the calculations as far as the trailing edge of the airfoil, it was necessary to modify slightly the Schlichting method by extrapolation of the curves in figures 5 and 6 of reference 8 beyond the value of  $k$  for which the Schlichting method breaks down. The recommendation of reference 8 that separation be assumed to exist when  $k$  equals  $-0.0682$  was ignored in order to avoid the contradiction that the boundary-layer profile can become more convex and, at the same time, approach separation.

Lin's approximate formula (reference 1) was used to calculate the Reynolds number  $R_{s,cr}$  at which any Schlichting velocity profile is neutrally stable. The stability theory as originally derived assumed that the boundary-layer thickness and velocity distribution did not vary with distance along the surface. Pretsch (reference 12), however, showed that the rates of variations in the thickness and velocity distribution which normally occur can have only a second-order effect on the stability. Lin's stability theory may be used, therefore, to calculate the stability of boundary layers in the presence of pressure gradients. When combined with the Schlichting method, Lin's formula becomes

$$R_{s,cr} = \frac{\left[1 - K \left(2 - \frac{\theta}{\pi}\right)\right] 25 \left(\frac{du/U}{d\eta}\right)_1}{u_c^4}$$

where  $u_c$  is equal to the value of  $u$  for which

$$-\pi \left(\frac{du/U}{d\eta}\right)_1 \left[3 - \frac{2 \left(\frac{du/U}{d\eta}\right)_\eta}{u/U}\right] \frac{u/U \left(\frac{d^2u/U}{d\eta^2}\right)}{\left(\frac{du/U}{d\eta}\right)^3} = 0.58$$

and where the subscript 1 denotes "at surface." The application of Lin's formula to the Schlichting profiles results in the curve of figure 9 which shows the variation of the critical Reynolds number  $R_{s,cr}$  with change in the Schlichting velocity-profile shape parameter  $K$ . In figure 10 are shown velocity profiles for three values of  $K$ .

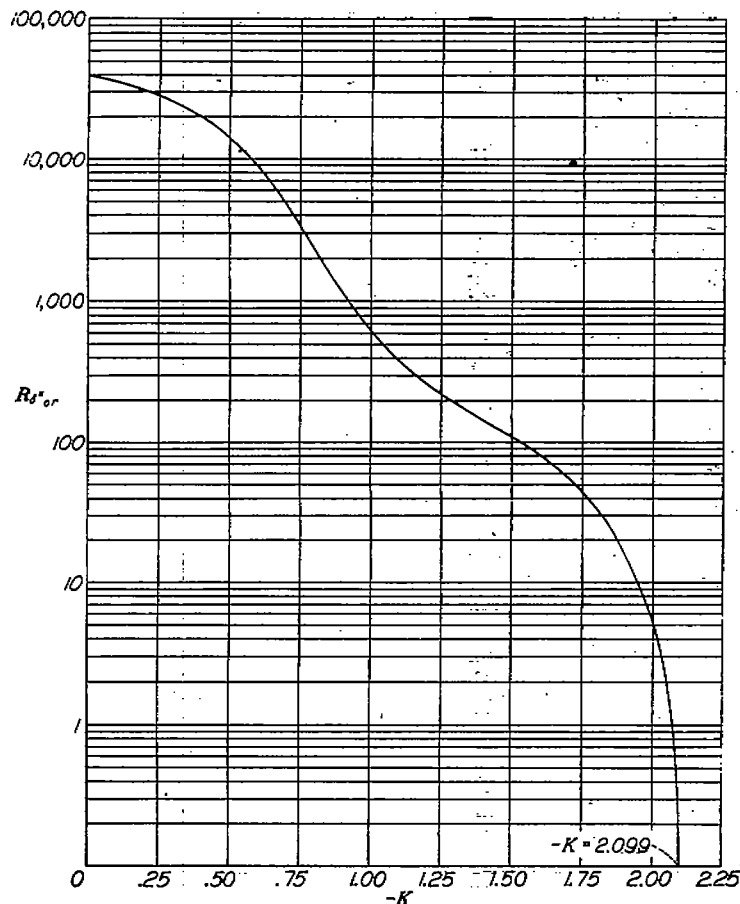


FIGURE 9.—Theoretical variation of critical boundary-layer Reynolds number with boundary-layer shape parameter.

A special procedure was used to calculate the distribution of the velocity of flow through the surface that was necessary to keep the boundary layer neutrally stable,  $R_s = R_{s,cr}$ . For these cases, suction was begun at the first station at which the boundary layer would become unstable without suction. The special method depends on the fact that the condition of neutral stability,  $R_{s,cr} = R_s$ , can be written as

$$R_{s,cr} = \frac{U}{U_0} \sqrt{z} \sqrt{R} \frac{\delta^*}{\theta}$$

or

$$\frac{R_{s,cr}}{\delta^*/\theta} = \phi(K) = \frac{U}{U_0} \sqrt{z} \sqrt{R}$$

where  $R_{s,cr}$ ,  $\frac{\delta^*}{\theta}$ , and  $\phi$  are functions only of  $K$ . The numerical value of the function  $\phi(K)$  depends on  $\frac{U}{U_0} \sqrt{z} \sqrt{R}$ . With a known value of  $z$  at the station at which suction begins,  $K$  can be found from the value of  $\frac{U}{U_0} \sqrt{z} \sqrt{R}$ . All the quantities necessary to proceed to the next station by the step-by-step integration process can be calculated once  $K$  is determined. The calculation of these quantities provides the value of the local-suction-velocity ratio  $v_0/U_0$ .

In figure 11 are presented the curves of  $R_s$  and  $R_{s,cr}$  as determined from the calculation for the suction flow required to keep the boundary layer neutrally stable at all points on the airfoil at a Reynolds number of  $15 \times 10^6$ . The calculated

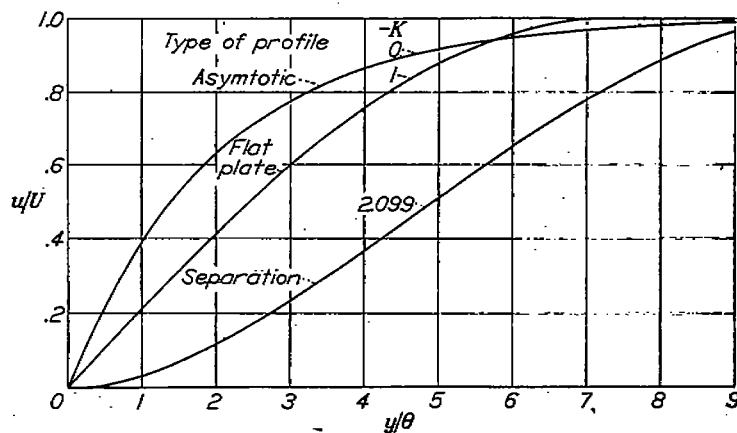


FIGURE 10.—Several boundary-layer profiles for values of shape parameter  $K$  as calculated by Schlichting.

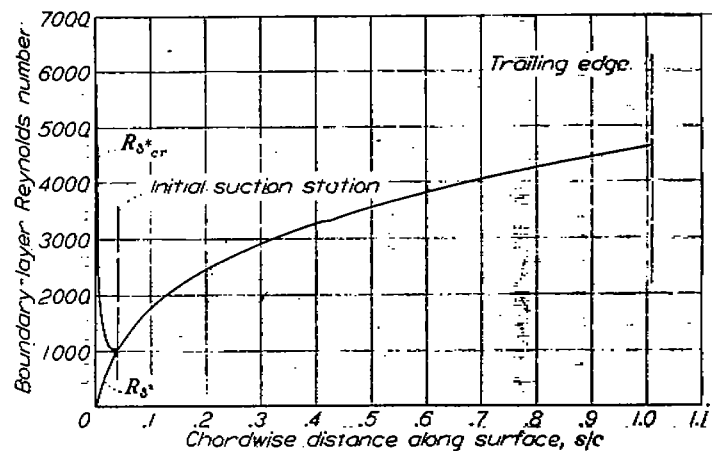


FIGURE 11.—Theoretical chordwise variation of boundary-layer Reynolds number on the NACA 64A010 airfoil for  $R_{s,cr} = R_s$ ;  $R = 15.0 \times 10^6$ ;  $C_0 = 0.000405$ ;  $\alpha = 0^\circ$ .

variation of  $v_0/U_0$  over one surface is shown in figure 12. The suction flow required to keep the boundary layer neutrally stable decreases slowly as the region of falling pressure on the airfoil surface is traversed. When the region of rising pressure is entered, the required suction rises rapidly and continues to increase to the trailing edge. The summary of the results of the computations for the minimum suction quantities is presented in figure 13.

In figure 14 are presented curves of  $R_{s,cr}$  and  $R_s$  for cases where  $v_0/U_0$  is the same over the entire surface. The figures illustrate that by a sufficient increase in the value of the suction parameter  $\frac{v_0}{U_0} \sqrt{R}$  the position at which the boundary layer first becomes unstable on the NACA 64A010 airfoil

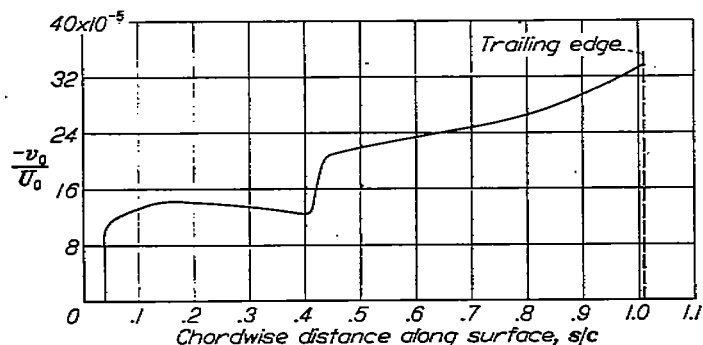


FIGURE 12.—Theoretical chordwise variation of minimum suction velocity ratio required to produce neutral stability at all points along the chord of the NACA 64A010 airfoil.  $R=15.0 \times 10^6$ ;  $\alpha_0=0^\circ$ ;  $C_d=0.000405$ .

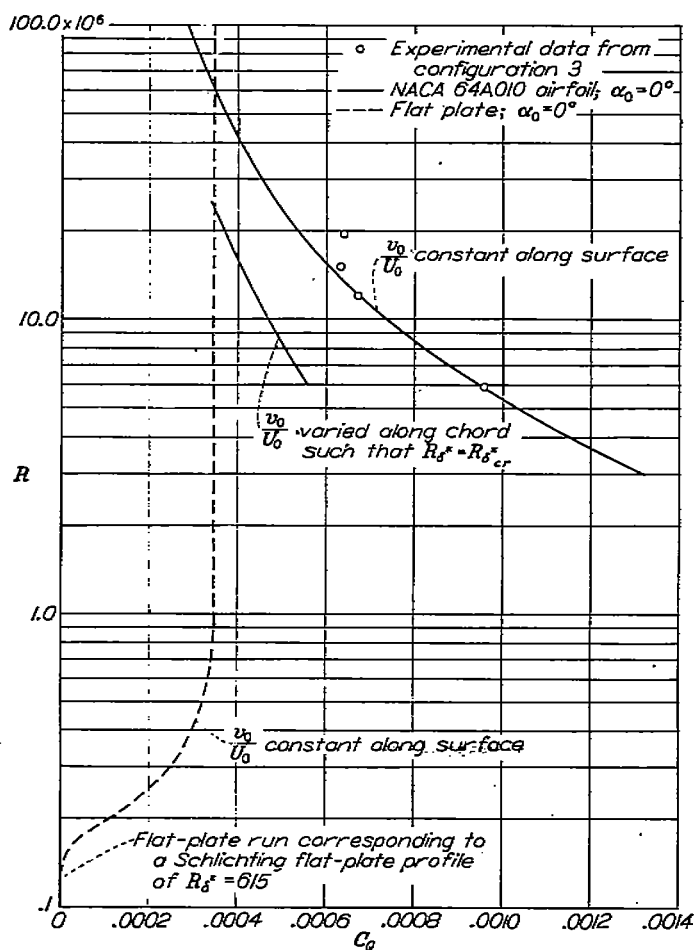


FIGURE 13.—Theoretical variation of free-stream Reynolds number with minimum suction-flow coefficient required to produce full-chord laminar stability.

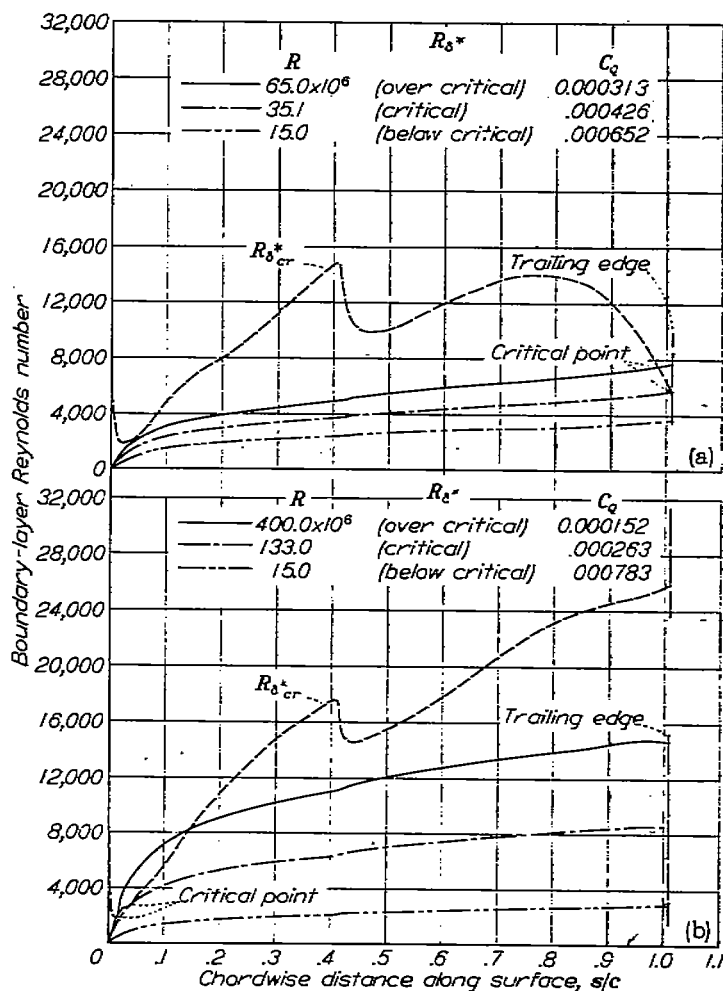
can be made to jump from the trailing edge to the region near the leading edge. It may be of interest to note from figure 14 (a) that the Reynolds number can be increased considerably and that the suction coefficient can be decreased appreciably without exposing much of the trailing surface to turbulent flow.

The curves of  $R_{s,cr}$  and  $R_s$  can be found at any Reynolds number, when they are known at one Reynolds number and one value of  $v_0/U_0$ , by noting that if  $\frac{v_0}{U_0} \sqrt{R}$  does not vary with Reynolds number then the  $R_{s,cr}$  curve is independent of Reynolds number and

$$\frac{R_{s,2}}{R_{s,1}} = \sqrt{\frac{R_2}{R_1}} \quad (1)$$

Thus, for a given distribution of  $\frac{v_0}{U_0} \sqrt{R}$ , which results in a fixed distribution of  $R_{s,cr}$ , the  $R_s$  curve for the same distribution of  $\frac{v_0}{U_0} \sqrt{R}$  but some other  $R$  can be found by equation (1).

At some value of  $R$ ,  $R_s$  will touch and yet not cross the  $R_{s,cr}$  curve at only one point. (See fig. 14.) This



(a) Critical point near trailing edge;  $\frac{v_0}{U_0} \sqrt{R}=1.25$ .

(b) Critical point near leading edge;  $\frac{v_0}{U_0} \sqrt{R}=1.50$ .

FIGURE 14.—Theoretical chordwise variation of boundary-layer Reynolds number and critical boundary-layer Reynolds number for the NACA 64A010 airfoil at three free-stream Reynolds numbers for constant chordwise inflow velocity.  $\alpha_0=0^\circ$ .

procedure results in one point on the curve of figure 13 which shows the variation of  $R$  with the minimum  $C_q$  required to produce full-chord laminar stability. Other points on the curve of figure 13 may be found by application of the foregoing procedure to other choices of  $\frac{v_0}{U_0} \sqrt{R}$  which result in other  $R_{cr}$  distributions.

Because the first theoretical studies of the effects of suction on boundary-layer stability were made for the flow over a flat plate, it was thought of interest to include the curve for the flat plate in figure 13 wherein it is illustrated that no suction is required to keep the flow stable on a flat plate when the Reynolds number is sufficiently low. This result is in contrast to that for the airfoil which, because of the adverse

pressure gradient over its rear portion, requires suction at all Reynolds numbers to maintain laminar flow to the trailing edge. Figure 13, however, indicates the rather surprising result that in order to keep full-chord laminar flow at large Reynolds numbers the NACA 64A010 airfoil requires smaller values of  $C_q$  than are required for a flat plate. This outcome seems reasonable because, near the leading edge where both the flat plate and the airfoil become critical at high Reynolds numbers, the airfoil profits from the existence of a favorable pressure gradient which increases the critical boundary-layer Reynolds number and decreases the actual boundary-layer Reynolds number over that of the flat plate for the same free-stream Reynolds number.

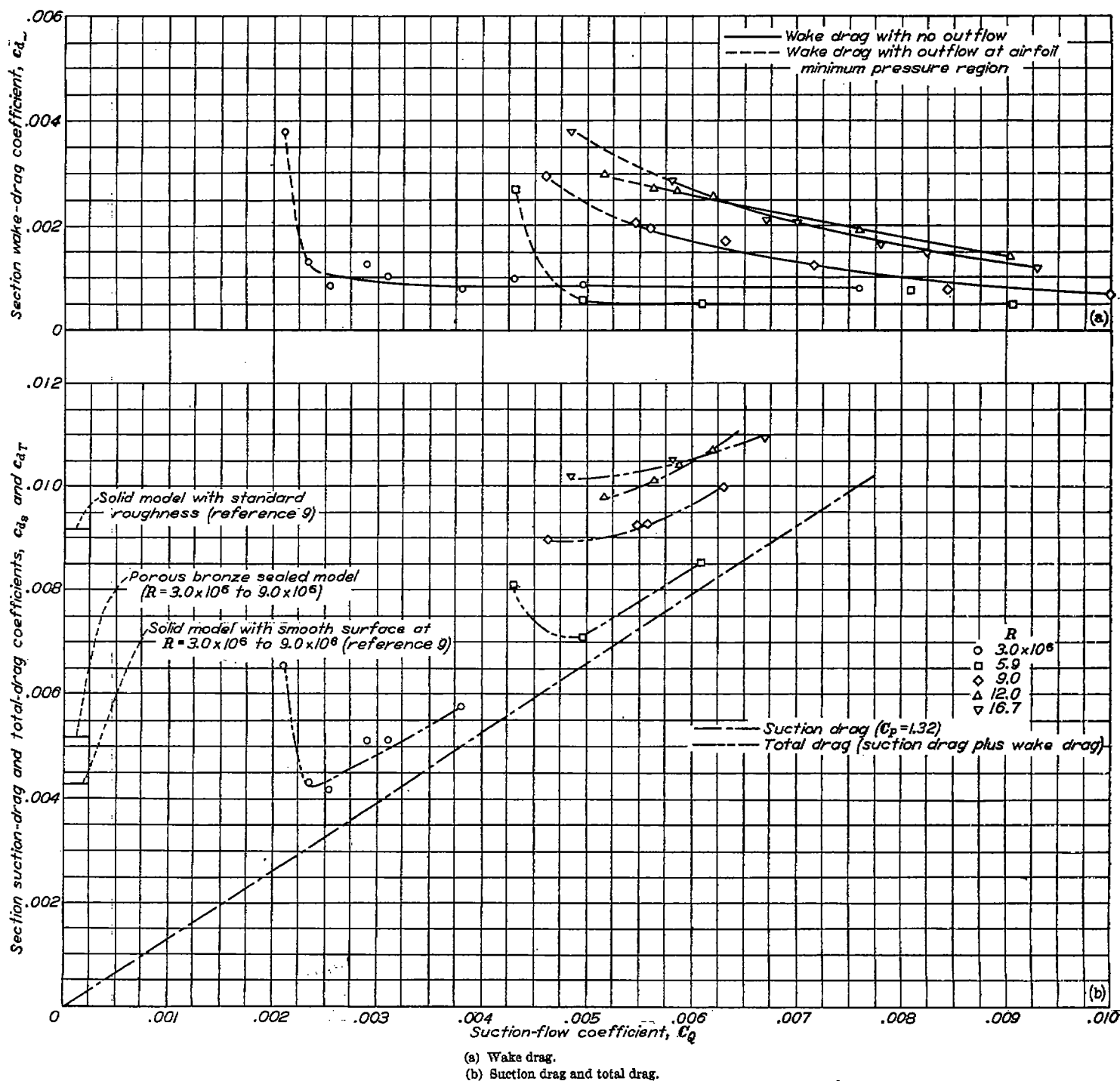


FIGURE 15.—Variation of section drag coefficients with suction-flow coefficient for porous bronze NACA 64A010 airfoil model.  $C_{\theta} = 7.2 \times 10^{-3}$ ;  $\alpha = 0^\circ$ ; configuration 1.

# EXPERIMENTAL CONFIGURATION 1

**Wake drag.**—The variation of section wake-drag coefficient with suction-flow coefficient is shown in figure 15(a) for Reynolds numbers up to  $16.7 \times 10^6$  for configuration 1. The static pressure in the interior of this model arrangement was everywhere the same.

At a Reynolds number of  $3.0 \times 10^6$  the section wake-drag coefficient for  $C_q > 0.0028$  was constant and equal to about 0.0008. For a Reynolds number of  $5.9 \times 10^6$  and for  $C_q > 0.0050$  the wake-drag coefficient remained practically constant at 0.0005. The wake drag at Reynolds numbers of  $9.0 \times 10^6$ ,  $12.0 \times 10^6$ , and  $16.7 \times 10^6$ , however, decreased steadily with increase in  $C_q$  but never became less than the lowest drags obtained at a Reynolds number of  $5.9 \times 10^6$ , even for a suction-flow coefficient as high as 0.010.

The rapid increase of  $c_{d_m}$  that occurred with decreasing  $C_q$  for values of  $C_q$  slightly less than 0.0024 at a Reynolds number of  $3.0 \times 10^6$  and for values of  $C_q$  less than about 0.0048 at a Reynolds number of  $5.9 \times 10^6$  was caused by a rapid forward shift of the point of transition from laminar to turbulent flow. The curves in figure 16 show that at 83 percent of the chord, at a Reynolds number of  $6.0 \times 10^6$ , the boundary layer on the upper surface was laminar for a  $C_q$  of 0.0048 but was turbulent for only a slightly lower  $C_q$  of 0.0046. Other boundary-layer surveys, not presented herein, indicated that, whenever a rapid increase in drag coefficient accompanied a small decrease in flow coefficient, the boundary layer changed rapidly from laminar to turbulent over a large portion of the surface.

Outflow through the surface occurred when the static pressure inside the skin was greater than the minimum static pressure on the outside of the airfoil. The curves of  $c_{d_m}$  against  $C_q$  are shown in figure 15 (a) as dash lines when outflow occurred locally and as solid lines when inflow occurred over the whole airfoil. At Reynolds numbers of  $3.0 \times 10^6$  and  $5.9 \times 10^6$  the values of minimum  $C_q$  required to prevent outflow are seen to be very near the value of  $C_q$  at which the drag changes rapidly. It seems probable that outflow produced the rapid forward shift of the transition point

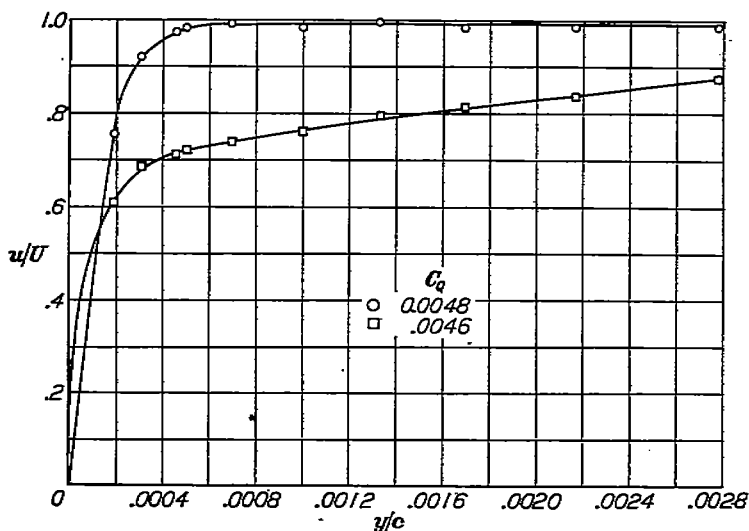


FIGURE 16.—Boundary-layer surveys for two values of suction-flow coefficient at station 0.83c on upper surface of porous bronze NACA 64A010 airfoil model. Configuration 1;  $R = 6.0 \times 10^6$ ;  $\alpha_1 = 0^\circ$ .

at least for Reynolds numbers up to  $5.9 \times 10^6$ . From the plots of  $c_{d_m}$  against  $C_q$  the lowest  $C_q$  for which no outflow occurred at each Reynolds number is seen to increase with increasing Reynolds number. This increase of the minimum value of  $C_q$  with Reynolds number is a result of the linear variation of flow velocity through the sintered bronze with pressure drop across the surface; the minimum  $C_q$  for no outflow increases with the free-stream Reynolds number. A more detailed treatment of this subject is presented in appendix A.

Wake-drag measurements for Reynolds numbers of  $9.0 \times 10^6$ ,  $12.0 \times 10^6$ , and  $16.7 \times 10^6$  as shown in figure 15 (a) indicated that laminar flow was probably not maintained over the complete chord of the model. The gradual decrease of wake-drag coefficient with increasing flow coefficient may have been caused either by a gradual rearward movement of the transition point with increasing flow coefficient or by a mere reduction in the size of the turbulent boundary layer. The extreme thinness of the boundary layer at these high Reynolds numbers prevented an accurate determination of its shape even near the trailing edge. It should be noted that full-chord laminar flow was not maintained even though the suction pressures were sufficient to prevent outflow. Theoretical calculations for a Reynolds number of  $16.7 \times 10^6$  for the configuration and inflow distribution tested indicated that the laminar boundary layer should have been very stable.

The basis for a possible explanation of the transition difficulties at the higher Reynolds number is indicated in reference 13. It is shown therein that the presence of a surface projection will cause premature transition of a laminar boundary layer when the Reynolds number based on the height of the projection and the velocity at the top of the projection exceeds a critical value that is dependent on the geometry of the projection.

Although the numerous protuberances on the bronze skin were sanded to very small dimensions, calculations indicated that the relatively large amount of suction near the leading edge of the model so thinned the boundary layer (especially at the higher Reynolds numbers) that even the particles forming the material probably projected completely through the boundary layer. Because of the high velocity at the top of the particles at the high Reynolds numbers, it seems entirely possible that the critical Reynolds number for the roughness was exceeded in spite of its small height, and thus large disturbances were introduced into the boundary-layer flow. The relatively high drag coefficients measured under such conditions of roughness show that the suction-type profile is not stable to sufficiently large disturbances. The relative stability of the suction-type and no-suction-type profiles to finite disturbances is an important problem for future research.

The difficulties associated with obtaining low drag at high values of the Reynolds number are seen from the foregoing discussion to result from nonuniformity of the chordwise inflow distribution (excessive suction near leading edge) and from the surface irregularities of the material. If the Reynolds number is increased by increasing the value of  $U_0/\nu$  while the size of the model is held constant, the inflow distribution becomes increasingly nonuniform (see equation (A4), appendix A) and the ratio of the size of the roughness

to the boundary-layer thickness increases. Both of these effects are unfavorable for obtaining low drag at high Reynolds numbers. On the other hand, if  $c_{v0}/t$  is held constant (no change in the type of material used) and if the Reynolds number is increased by increasing the chord of the model, the inflow distribution will remain unchanged but the ratio of the size of the roughness to the boundary-layer thickness will vary inversely as the square root of the Reynolds number. For this reason, it seems likely that favorable results can be obtained more easily with a large model than with a small one.

**Total drag.**—The measured pressure-loss coefficient for the suction air was used to calculate the section suction-drag coefficient and the results are shown in figure 15 (b). The suction-drag coefficient based on the model chord was calculated as  $C_P \times C_Q$ , which is the drag equivalent of the power required to pump the suction air back to free-stream total pressure. (See appendix B.) In this method of calculating suction drag, the over-all pumping efficiency is considered to be equal to that of the main propulsive system.

As may be seen in figure 15 (b), the variation of  $c_d$  was assumed to be linear with  $C_Q$  for all Reynolds numbers because of the small variation in  $C_P$  which averaged about 1.32. Inasmuch as there is no induced drag on a two-dimensional model, the total drag is the sum of the suction and wake drags. As shown in figure 15 (b), the minimum total drag at a Reynolds number of  $3.0 \times 10^6$  occurred at a  $C_Q$  of about 0.0024, which was slightly less than the minimum  $C_Q$  required to prevent outflow; the minimum total-drag coefficient of 0.0042 is an inappreciable improvement over 0.0043, the drag coefficient of a solid NACA 64A010 airfoil with a smooth and faired surface at a Reynolds number of  $3.0 \times 10^6$  (shown in figure 15 (b) as taken from reference 9). The porous model, however, did not have a completely smooth and faired surface, and a test made with the surface sealed resulted in a no-suction-drag coefficient of approximately 0.0052. The value of 0.0052 is probably somewhat low inasmuch as the surface was sealed with external applications of water glass and wax; as a result, the surface texture was unavoidably improved over that for the unsealed condition although the waviness of the surface was probably not affected. The no-suction-drag coefficient, therefore, would probably be somewhat greater than 0.0052 but less than 0.0092, the value for the extreme condition of standard leading-edge roughness on the solid airfoil (reference 9). The minimum total-drag coefficient increased with increasing Reynolds number with the result that, at a Reynolds number only slightly greater than  $3.0 \times 10^6$ , no decrease in total drag was obtained by suction. A large proportion of the total drag consisted of suction drag because of the excessive amounts of air required at the leading-edge and trailing-edge surfaces of the airfoil in order to prevent outflow at the minimum pressure point.

The total amount of air that needs to be withdrawn in order to prevent outflow can be greatly reduced by applying suction separately to small portions of the airfoil surface. This purpose was accomplished by dividing the underskin region into separate compartments (configuration 2) as described previously in the section entitled "Model."

#### CONFIGURATION 2

**Wake drag.**—Wake-drag tests made on the compartmented model (configuration 2) previous to the tests reported herein indicated that the nose should be sealed for about 1 inch back from the leading edge (fig. 4) in order to obtain low drags at reasonable suction coefficients. The character of the flow at the leading edge before the nose was sealed was not clearly established, but early transition probably occurred because of excessive local outflow near the nose where the external-pressure variation over the first compartment was very large. A better understanding of these outflow difficulties may be gained from the discussion on compartmentation in appendix A.

As shown in figure 17 (a), the section wake-drag coefficient for the model with sealed nose and compartments was less than 0.0010 (for Reynolds numbers as high as  $7.8 \times 10^6$ ) for suction-flow coefficients that ranged from 0.0015 at a Reynolds number of  $3.0 \times 10^6$  to about 0.0035 at a Reynolds number of  $7.8 \times 10^6$ . At a Reynolds number of  $9.1 \times 10^6$  the wake drag remained greater than 0.0030 even for flow coefficients as high as 0.0040. Failure to obtain lower wake drags was believed to result from the presence of outflow. Although no outflow and low wake drags might have been obtained at higher suction-flow coefficients, the total drag would not have been reduced because of the excessive suction drags that would have resulted from the large suction quantities.

A comparison of figures 15 (a) and 17 (a) indicates that for equal Reynolds numbers the minimum suction-flow coefficients for which low wake drags were obtained for the compartmented model were about one-third of those required for configuration 1. The largest Reynolds number at which low drag occurred was also extended by compartmenting the model. Thus, low wake drags might be obtained at Reynolds numbers higher than  $7.8 \times 10^6$  and at suction-flow coefficients lower than 0.0035 if the chordwise distribution of suction were further controlled.

**Total drag.**—Throughout the low-drag range the average total-pressure loss in the suction air for the compartmented model corresponded to an average pressure-loss coefficient of about 1.40. This average loss coefficient was used to compute the suction-drag coefficient that could be expected for an airfoil compartmented in the same manner as the model tested. The sum of the wake and suction drags is shown in figure 17 (b). At Reynolds numbers of  $3.0 \times 10^6$  and  $5.9 \times 10^6$  the minimum  $c_{dt}$  was about 0.0028. At

higher Reynolds numbers the minimum  $c_{dT}$  was larger because of the larger  $C_Q$  necessary for low wake drags. In spite of the larger  $C_Q$  at a Reynolds number of  $7.8 \times 10^6$ , the minimum total-drag coefficient, 0.0048, was only slightly greater than the drag coefficient for the smooth solid-surface model of the same contour (reference 9) and somewhat

less than the drag coefficient for the porous bronze model with the skin entirely sealed to suction.

The over-all gain in compartmenting the model may be seen by comparing the total drags in figures 15 (b) and 17 (b) from which it is seen that at a Reynolds number of  $5.9 \times 10^6$  the total drag of the compartmented model (configuration 2)

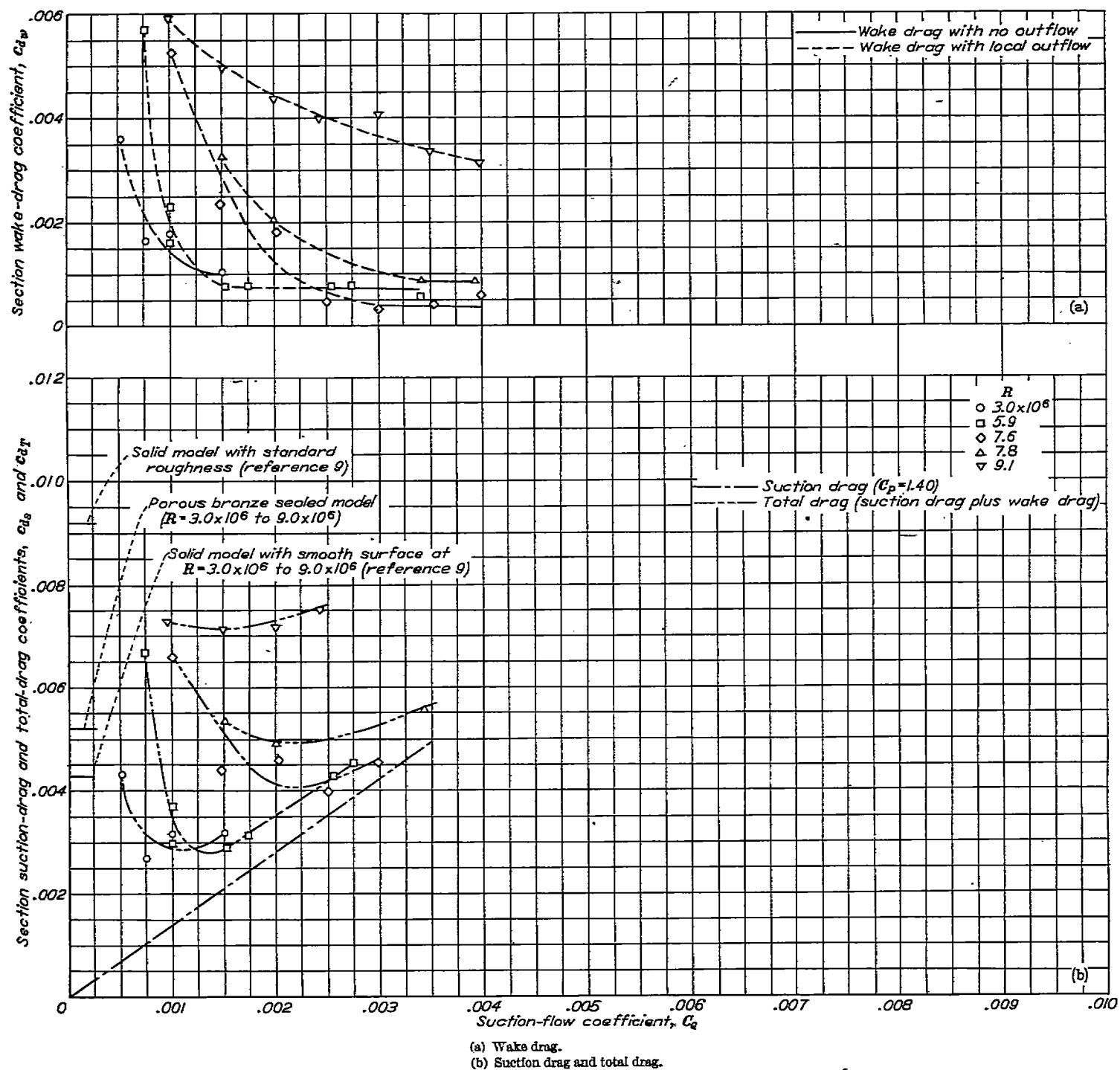


FIGURE 17.—Variation of section drag coefficients with suction-flow coefficient for porous bronze NACA 64A010 airfoil model.  $\frac{c_{rs}}{c_l} = 7.2 \times 10^{-4}$ ;  $\alpha = 0^\circ$ ; configuration 2.

was only 40 percent of that for the uncompartmented model (configuration 1). In an attempt to improve further the chordwise inflow distribution and thus to obtain full-chord laminar flow and reductions in total drag at larger values of the Reynolds number, the model was equipped with a porous sintered-bronze surface of much lower porosity (configuration 3) as described previously in the section entitled "Model."

### CONFIGURATION 3

**Wake drag.**—The leading edge of this model configuration was sealed to the 5-percent-chord station, which is approximately the chordwise station ahead of which no suction is required theoretically to maintain the boundary-layer

Reynolds number less than the critical value for all test Reynolds numbers anticipated (figs. 11 and 14). The section wake-drag coefficients are plotted against suction-flow coefficient in figure 18 (a) for Reynolds numbers from  $5.9 \times 10^6$  to  $19.8 \times 10^6$ . The static pressure in the interior of this model arrangement was everywhere the same as it was for the case of configuration 1.

The variation of drag coefficient with suction-flow coefficient  $C_q$  is similar for all Reynolds numbers investigated; that is, an abrupt decrease in drag coefficient to a value of about 0.0008 occurs at some critical value of  $C_q$  dependent upon the Reynolds number and is followed by a much more gradual decrease with an increase in  $C_q$ . Full-chord

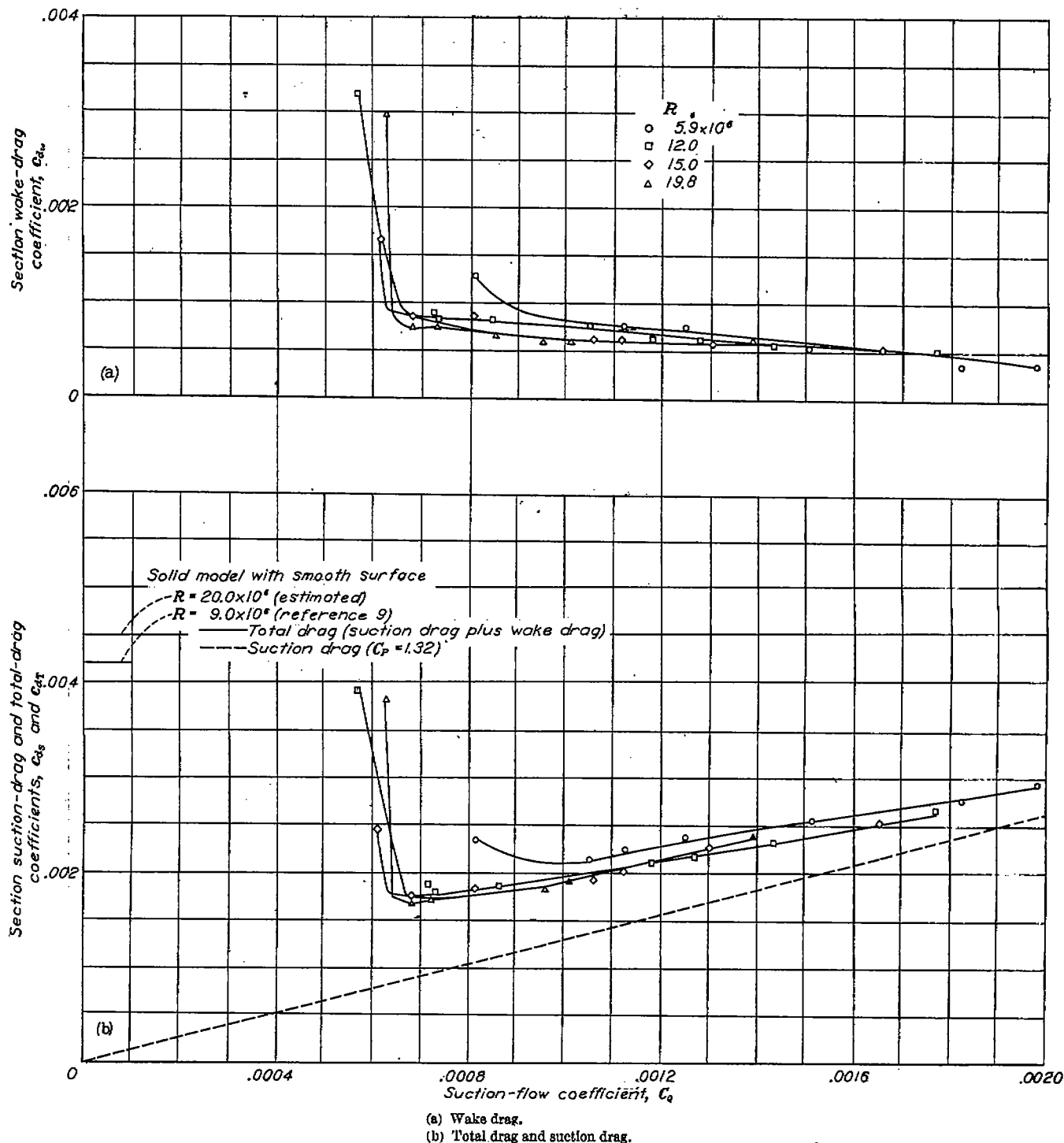


FIGURE 18.—Variation of section drag coefficients with suction-flow coefficient for porous bronze NACA 64A010 airfoil model.  $\frac{C_{d_s}}{C_l} = 2.33 \times 10^{-4}$ ;  $\alpha = 0^\circ$ ; configuration 3.

laminar flow is indicated for all values of wake-drag coefficient of about 0.0008 or less, inasmuch as boundary-layer profiles measured during tests of configuration 1 indicated that the boundary layer changed rapidly from turbulent over a large portion of the airfoil to laminar over virtually the full chord whenever a large decrease in drag accompanied a small increase in flow coefficient. The gradual reduction in drag with a further increase in  $C_Q$  above the value at which the large drag change occurs corresponds only to a progressive thinning of the full-chord laminar boundary layer. For the tests of configurations 1 and 2, the sudden forward movement in point of transition from laminar to turbulent flow with a small decrease in  $C_Q$  was caused by outflow of air through the surface when the static pressure inside the skin was greater than the minimum static pressure on the outside of the airfoil. For the tests of configuration 3, however, the skin was dense enough so that no outflow of air occurred for all values of  $C_Q$  investigated at Reynolds numbers up to at least  $15 \times 10^6$ .

The probable cause of the rapid increase in drag and corresponding forward movement of transition observed in the tests of configuration 3 at Reynolds numbers up to  $15 \times 10^6$  is revealed by a comparison of the values of  $C_Q$  at which the rapid drag rises occurred (fig. 18 (a)) with the minimum theoretical values of  $C_Q$  required to keep the laminar boundary layer stable. The experimental values of  $C_Q$  at which the rapid drag rises occurred for configuration 3 are plotted in figure 13 for ease of comparison. The minimum experimental values of  $C_Q$  for full-chord laminar flow are of the same order of magnitude as the theoretical values and decrease with an increase in Reynolds number in the same manner as the theoretical up to a Reynolds number of  $15 \times 10^6$ . No outflow of air is known to have existed up to a Reynolds number of  $15 \times 10^6$  and because of the sealed nose which prevented excessive suction at the leading edge and the especially smooth surface of this model configuration, it is believed that roughness did not cause transition at the low values of  $C_Q$ ; therefore, the sudden drag rise probably occurred when the suction became insufficient (at least over a portion of the airfoil chord) to stabilize the laminar boundary layer. At a Reynolds number of  $19.8 \times 10^6$  outflow of air rather than insufficient suction is likely to have caused the rapid drag rise with a decrease in  $C_Q$ . For the porous bronze skin used in the tests of configuration 3, a value of  $C_F$  equal to 1.32 was measured at a value of  $C_Q$  of about 0.0007 at a Reynolds number of  $19.8 \times 10^6$ . The minimum local pressure on the airfoil exterior when mounted in the wind tunnel corresponds to a value of pressure coefficient  $S$  equal to about 1.31. Inasmuch as  $C_F$  decreases with a decrease in  $C_Q$ , a value of  $C_Q$  slightly lower than 0.0007 would result in outflow of air through the surface and forward movement in transition from laminar to turbulent flow.

The maximum Reynolds number at which recorded data were obtained was  $19.8 \times 10^6$ . During the tests, however, at a value of  $C_Q$  less than 0.001, full-chord laminar flow was maintained up to a Reynolds number of about  $24 \times 10^6$  as evidenced by a visual observation of the drag manometer which indicated values of the drag coefficient of about 0.0006. Unfortunately, however, a sudden change in the model occurred before any data could be recorded. It was

found that the bronze skin had buckled to such an extent that it was impossible to repeat the full-chord laminar-flow tests at Reynolds numbers somewhat lower than  $20 \times 10^6$ , although before the skin took the permanent set, repetition of the low-drag results could be made.

**Total drag.**—The dashed curve of figure 18 (b) represents the variation of  $c_{a_r}$  with  $C_Q$  for an assumed constant value of  $C_F$  equal to 1.32. This value of  $C_F$  was chosen in order to present an indication of the minimum suction-drag coefficient required to maintain full-chord laminar flow at any value of the suction-flow coefficient and Reynolds number. As pointed out in the previous section entitled "Wake drag" a value of  $C_F$  slightly lower than 1.32 would result in outflow of air through the surface near the 0.40c position and a forward movement in the position of transition. The curves of section total-drag coefficient plotted against  $C_Q$  (fig. 18 (b)) are the sums of the suction and wake drags. The minimum section total-drag coefficient decreased with an increase in Reynolds number because of the decrease in  $C_Q$  required to obtain low wake drags. At a Reynolds number of  $19.8 \times 10^6$  the minimum  $c_{a_r}$  was 0.0017 as compared with a value of about 0.0045 (estimated from data of reference 14) for an NACA 64A010 airfoil without boundary-layer control at a Reynolds number of  $20 \times 10^6$ .

#### COMPARISON BETWEEN THEORY AND EXPERIMENT

The theoretical variations of  $R_{i^*}$ ,  $R_{i^*_{cr}}$ , and  $v_0/U_0$  with  $s/c$  cannot be compared with experiment because local inflow velocities and boundary-layer velocity profiles were not measured. The theoretical total-suction quantities can, however, be compared with the total-suction quantities at the knees of the curves of wake-drag coefficient against suction-flow coefficient.

The following table contains the results of the comparison between theory and experiment:

R	Minimum values of $C_Q$ for laminar stability				
	Theoretical		Experimental		
	Neutral stability	Constant inflow	Configuration 1	Configuration 2	Configuration 3
$3.0 \times 10^6$	-----	0.00132	0.0025	0.0015	-----
5.9	0.00058	0.00096	0.0018	0.0015	0.00096
7.6	0.00051	0.00084	-----	0.0024	-----
7.8	0.00051	0.00083	-----	0.0034	-----
9.0	0.00048	0.00077	0.0100	-----	-----
12.0	0.00044	0.00067	-----	-----	0.00087
15.0	0.00041	0.00060	-----	-----	0.00063
19.8	0.00037	0.00054	-----	-----	0.00064

Although the chordwise inflow distribution for configuration 3 was more uniform than for either of the previous configurations and although the minimum experimental values of  $C_Q$  for laminar stability agree very closely with the theoretical values of  $C_Q$  for a constant chordwise inflow, the close agreement cannot be construed as a quantitative check of the theory inasmuch as it is known that the experimental chordwise inflow distribution was not constant.

As shown in the table the minimum experimental values of  $C_Q$  for low wake drags for configurations 1 and 2 were appreciably greater than the theoretical values and also increased with an increase in free-stream Reynolds number in contrast to the trend indicated by the theory. This experimental

variation of minimum  $C_q$  with Reynolds number for configurations 1 and 2 was shown previously to be a result of outflow of air through the surface and the fact that the minimum  $C_q$  for incipient outflow increases with the Reynolds number. (See appendix A.) When it became possible to attain lower values of  $C_q$  for incipient outflow at a given Reynolds number by means of the dense skin of configuration 3, the minimum values of  $C_q$  became of the same order of magnitude as the theoretical values and had the same trend with Reynolds number as predicted by theory; that is, the minimum  $C_q$  decreased with an increase in Reynolds number up to the maximum test Reynolds number at which outflow of air once again prevented a further decrease in  $C_q$  for full-chord laminar flow. It appears, therefore, that the theoretical concepts with regard to area suction are valid; the Reynolds number itself, then, should not be a limiting parameter in attainment of full-chord laminar flow provided that the airfoil surfaces are kept sufficiently smooth and fair and provided that outflow of air through the surface is prevented.

Quantitative information on the effects of surface roughness or fairness on the stability of the laminar boundary layer, however, is not yet available although some indications of adverse effects of roughness on the ability to maintain full-chord laminar flow were discussed previously. Another indication of the adverse effects of surface roughness was obtained during a preliminary test run on configuration 1 before the model surfaces were sanded.

For this condition, numerous protuberances existed of sufficient magnitude to cause premature transition of the boundary layer at a Reynolds number as low as  $3.0 \times 10^6$ . It is possible, however, that the excessive suction at and near the model leading edge may have unduly decreased the boundary-layer thickness relative to the size of the projections; thus, the sensitivity of the boundary layer to the existing disturbances was unnecessarily increased. This explanation, as discussed previously, was prompted by the work of reference 13. Although surface roughness did not appear to cause transition on the sealed-nose configurations (configurations 2 and 3) for the combinations of Reynolds numbers

and flow rates that were tested, it is believed that with other combinations of Reynolds numbers and suction rates (at least for the same model) the boundary layer could become thin enough to allow the surface roughness to cause transition. More information on the effects of area suction on the stability of the laminar boundary layer in the presence of surface disturbances is still required before it can be determined whether area suction can be made practical for the control of the laminar boundary layer.

### CONCLUDING REMARKS

Results were presented of a low-turbulence wind-tunnel investigation of an NACA 64A010 airfoil with porous surfaces of sintered bronze. Full-chord laminar flow was maintained by the application of area suction up to a Reynolds number of  $19.8 \times 10^6$ . At a Reynolds number of  $19.8 \times 10^6$ , the total-drag coefficient (wake drag plus the drag equivalent of the suction power required) was equal to 0.0017 as compared with an estimated value of 0.0045 for a smooth and fair NACA 64A010 airfoil without boundary-layer control at a Reynolds number of  $20 \times 10^6$ . The minimum experimental values of suction-flow coefficient for full-chord laminar flow were of the same order of magnitude as the theoretical values and decreased with an increase in Reynolds number in the same manner as the theoretical values. It seems likely from the results that attainment of full-chord laminar flow by means of continuous suction through a porous surface will not be precluded by a further increase in Reynolds number provided that the airfoil surfaces are maintained sufficiently smooth and fair and provided that outflow of air through the surface is prevented. Further research is required, however, to determine quantitatively the effect of finite disturbances on the stability of suction-type velocity profiles.

LANGLEY AERONAUTICAL LABORATORY,  
NATIONAL ADVISORY COMMITTEE FOR AERONAUTICS,  
LANGLEY FIELD, VA., March 30, 1951.

## APPENDIX A

### SINTERED-BRONZE SUCTION REQUIREMENTS FOR THE CASE OF INCIPIENT LOCAL OUTFLOW

Several important conclusions may be drawn from a study of the conditions that cause local outflow through a porous sintered-bronze sheet installed on an airfoil as a boundary-layer suction surface. Outflow occurs through any point on the skin where the local static pressure on the inside of the skin is greater than the local external static pressure despite the existence of a difference in pressures at all other points such as to produce inflow. An internal pressure just low enough to prevent outflow at some critical point produces an average value of area suction-flow coefficient which depends on the porosity characteristics of the material.

For a given type of sintered bronze, the velocity into the surface varies directly as the pressure drop across the surface and inversely as the thickness of the sheet and the absolute viscosity of the fluid; thus,

$$v_0 = -\frac{c_{v_0} \Delta p}{\mu t} \quad (A1)$$

A dimensional analysis will show that the factor  $c_{v_0}$  has the dimensions of length<sup>2</sup>. This length is related to the effective diameter of the passages leading through the material. So long as the flow is of the purely viscous type, the value of  $c_{v_0}$  for a specific piece of porous material may be expected to be independent of the physical characteristics of the fluid passing through the material—that is, the viscosity and density.

Inasmuch as the suction-drag coefficient increases directly as the suction-flow coefficient  $C_Q$  (see appendix B), it is of interest to note the manner in which the porosity relation, equation (A1), affects the minimum  $C_Q$  necessary to prevent outflow. The average area suction-flow coefficient for both sides of a two-dimensional airfoil may be written as

$$C_Q = \frac{Q}{U_0 c b} = -\frac{\oint b v_0 ds}{U_0 c b} \quad (A2)$$

where the quantity of suction air is obtained by integrating the inflow velocity  $v_0$  over both upper and lower surfaces as indicated by the line integral sign. The inflow velocity given by equation (A1) may be rewritten as

$$v_0 = -\left(\frac{c_{v_0} q_0}{\mu t}\right) \left[ \left(\frac{H_0 - H_i}{q_0}\right) - \left(\frac{H_0 - p}{q_0}\right) \right] \quad (A3)$$

where  $H_i$  is equal to the internal static pressure because the internal velocity, and therefore the dynamic pressure, is extremely low. The two relations in equation (A3),  $\frac{H_0 - H_i}{q_0}$  and  $\frac{H_0 - p}{q_0}$ , are the suction pressure-loss coefficient and the external airfoil pressure coefficient, respectively. The inflow velocity at any point is now

$$v_0 = -\frac{c_{v_0} q_0}{\mu t} (C_P - S)$$

or

$$\frac{v_0}{U_0} = -\frac{c_{v_0}}{2ct} R (C_P - S) \quad (A4)$$

The suction-flow coefficient for the whole wing can now be written as

$$C_Q = -\frac{c_{v_0} R}{2ct} \oint (C_P - S) d\frac{s}{c} \quad (A5)$$

It may be seen by equation (A5) that, if conditions of airfoil pressure coefficient and suction pressure-loss coefficient remain fixed for a given porous-skin model wherein  $c_{v_0}$ ,  $t$ , and  $c$  are fixed, the value of  $C_Q$  to be associated with a given value of  $\oint (C_P - S) d\frac{s}{c}$  will vary linearly with  $R$ . Thus, for the outflow value of the integral where  $C_P$  equals  $S$  at some point on the airfoil and is higher at all other points, the value of  $C_Q$  corresponding to outflow will increase linearly with increasing  $R$ , a result approximately in agreement with experimental results.

In order to have like test conditions for like Reynolds number as  $\rho$ ,  $U_0$ ,  $c$ , and  $\mu$  are varied, it is necessary that  $c_{v_0}/t$  vary directly with  $c$ . When models of different chords are geometrically similar to the extent that  $t$  is proportional to  $c$ , then  $c_{v_0}$  must vary directly as  $c^2$ . This result would be expected since it means that the effective diameter of the passage must vary directly as the chord; that is, the geometrical similarity must include the detailed geometry of the structure of the porous material, as well as the over-all dimensions of the model.

For like airfoils of different chords covered with the same porous material, equation (A4) indicates that the inflow

distribution at any chordwise position is unchanged if  $R$  is proportional to  $c$ —that is, if  $U_0/\nu$  is a constant. Thus, if the same airfoil profile were used throughout the span of a tapered wing and the wing were entirely covered with the same porous material, the inflow distribution would be similar for all sections of the tapered wing for the convenient condition of a constant suction pressure within the wing.

Compartmentation of an area-suction model can be used as a method for improving the chordwise inflow distribution so that excessive suction flows will not occur at any point, but, if this method is used, each compartment must be considered as a source of outflow. The flow removed through each compartment can be decreased by decreasing the pressure drop across the porous surface with a throttling device; and thus the effective  $C_p$  based on the static pressure in the compartment becomes less for no outflow than the  $C_p$  that would be required at the point of maximum  $S$  on the airfoil. (See fig. 2.) The net result of compartmenting the whole airfoil is

that for no outflow the sum of the incremental values of  $C_q$  for each compartment will be less than the minimum  $C_q$  required for no outflow for the uncompartmented model; furthermore, the greater the number of compartments, the greater is the decrease in the value of total  $C_q$  for incipient outflow. The end point of more and more compartments is that the chordwise inflow distribution can be set to any value desired. The greatest difficulty in compartmenting is experienced at and near the nose where even very small compartments must combat a very high chordwise change in pressure drop and thus of inflow distribution because of large variations in the external pressure. Inasmuch as extreme compartmentation may result in an immense construction problem, it may be more desirable to provide a skin which has a chordwise variation of porosity that will produce the desired inflow distribution. Such a skin could be obtained by a chordwise variation of either the thickness or the density of the material.

## APPENDIX B

### DETERMINATION OF SUCTION-DRAG COEFFICIENT

If it is assumed that the suction air is pumped back to free-stream total pressure by a blower and duct system which together have an efficiency of  $\eta_s$ , then the power required may be written as

$$P = \frac{Q(H_0 - H_i)}{\eta_s}$$

where  $H_i$  is the average total pressure of the suction as measured at a point under the surface of the wing and  $H_0$  is the free-stream total pressure.

If the flow quantity is expressed as the suction-flow coefficient

$$C_q = \frac{Q}{U_0 b c}$$

and the total pressure defect is expressed as a pressure-loss coefficient

$$C_p = \frac{H_0 - H_i}{q_0}$$

then the power may be written as

$$P = \frac{C_q U_0 b c C_p q_0}{\eta_s} \quad (B1)$$

If this amount of power were to be supplied by the airplane propulsive system of efficiency  $\eta_p$ , then the equivalent drag to be associated with this power could be written as

$$D = \frac{P \eta_p}{U_0}$$

or

$$c_{d, bcq_0} = \frac{P \eta_p}{U_0} \quad (B2)$$

where the equivalent drag is expressed in terms of a suction-drag coefficient based on the area of the wing.

Equations (B1) and (B2) permit the suction-drag coefficient to be expressed as

$$c_{d, bcq_0} = C_q C_p \frac{\eta_p}{\eta_s}$$

On the condition that the blower system operates as efficiently as the propulsive system, the suction-drag coefficient reduces to

$$c_{d, bcq_0} = C_q C_p \quad (B3)$$

### REFERENCES

1. Lin, C. C.: On the Stability of Two-Dimensional Parallel Flows. Part I.—General Theory. *Quarterly Appl. Math.*, vol. III, no. 2, July 1945, pp. 117-142; Part II.—Stability in an Inviscid Fluid. vol. III, no. 3, Oct. 1945, pp. 218-234; Part III.—Stability in a Viscous Fluid. vol. III, no. 4, Jan. 1946, pp. 277-301.
2. Schubauer, G. B., and Skramstad, H. K.: Laminar-Boundary-Layer Oscillations and Transition on a Flat Plate. NACA Rep. 909, 1948.
3. Schlichting, H.: The Boundary Layer of the Flat Plate under Conditions of Suction and Air Injection. R. T. P. Translation No. 1753, British Ministry of Aircraft Production. (From *Luftfahrtforschung*, Bd. 19, Lfg. 9, Oct. 20, 1942, pp. 293-301.)
4. Iglisch, Rudolf: Exakte Berechnung der laminaren Grenzschicht an der längsangeströmten ebenen Platte mit homogener Absaugung. *Schriften der Deutschen Akademie der Luftfahrtforschung*, Bd. 8B, Heft 1, 1944. (Also available as NACA TM 1205, 1949.)
5. Pretsch, J.: Die Leistungsparsnis durch Grenzschichtbeeinflussung beim Schleppen einer ebenen Platte. UM Nr. 3048, Deutsche Luftfahrtforschung (Berlin-Adlershof), 1943.
6. Schlichting, H.: Berechnung der laminaren Reibungsschicht mit Absaugung. *Forschungsbericht Nr. 1480*. Deutsche Luftfahrtforschung (Berlin-Adlershof), 1941.
7. Ulrich, A.: Theoretical Investigation of Drag Reduction in Maintaining the Laminar Boundary Layer by Suction. NACA TM 1121, 1947.
8. Schlichting, H.: An Approximate Method for Calculation of the Laminar Boundary Layer with Suction for Bodies of Arbitrary Shape. NACA TM 1216, 1949.
9. Loftin, Laurence K., Jr.: Theoretical and Experimental Data for a Number of NACA 6A-Series Airfoil Sections. NACA Rep. 903, 1948.
10. Von Doenhoff, Albert E., and Abbott, Frank T., Jr.: The Langley Two-Dimensional Low-Turbulence Pressure Tunnel. NACA TN 1283, 1947.
11. Von Doenhoff, Albert E.: Investigation of the Boundary Layer about a Symmetrical Airfoil in a Wind Tunnel of Low Turbulence. NACA ACR, Aug. 1940.
12. Pretsch, J.: Die Stabilität einer ebenen Laminarströmung bei Druckgefälle und Druckanstieg. *Jahrb. 1941 der deutschen Luftfahrtforschung*, R. Oldenbourg (Munich), pp. I 158-I 175.
13. Loftin, Laurence K., Jr.: Effect of Specific Types of Surface Roughness on Boundary-Layer Transition. NACA ACR L5J29a, 1946.
14. Loftin, Laurence K., Jr., and Bursnall, William J.: The Effects of Variations in Reynolds Number between  $3.0 \times 10^6$  and  $25.0 \times 10^6$  upon the Aerodynamic Characteristics of a Number of NACA 6-Series Airfoil Sections. NACA TN 1773, 1948.